Electronic Supplementary Material (ESI) for Physical Chemistry Chemical Physics.

Supplemental Information: Relevance of hydrogen bonded associates on the transport properties and nanoscale dynamics of liquid and supercooled 2-propanol

Yanqin Zhai
Department of Nuclear, Plasma, and Radiological Engineering, University of Illinois at Urbana-Champaign, Urbana, Illinois 61801, USA and Beckman Institute for Advanced Science and Technology, University of Illinois at Urbana-Champaign, Urbana, Illinois 61801, USA

Peng Luo
Beckman Institute for Advanced Science and Technology, University of Illinois at Urbana-Champaign, Urbana, Illinois 61801, USA

Michihiro Nagao
NIST Center for Neutron Research, National Institute of Standards and Technology, Gaithersburg, Maryland 20899, USA Center for Exploration of Energy and Matter, Indiana University, Bloomington, Indiana 47408, USA and Department of Physics and Astronomy, University of Delaware, Newark, Delaware 19716, USA

Kenji Nakajima, Tatsuya Kikuchi, and Yukinobu Kawakita
J-PARC Center, Japan Atomic Energy Agency, Tokai, Ibaraki 319-1195, Japan

Paul A. Kienzle and Antonio Faraone*
NIST Center for Neutron Research, National Institute of Standards and Technology, Gaithersburg, Maryland 20899, USA

Y Z†
Department of Nuclear, Plasma, and Radiological Engineering, University of Illinois at Urbana-Champaign, Urbana, Illinois 61801, USA Beckman Institute for Advanced Science and Technology, University of Illinois at Urbana-Champaign, Urbana, Illinois 61801, USA and Department of Electrical and Computer Engineering, University of Illinois at Urbana-Champaign, Urbana, Illinois 61801, USA
(Dated: February 25, 2021)

* antonio.faraone@nist.gov
† zhyang@illinois.edu

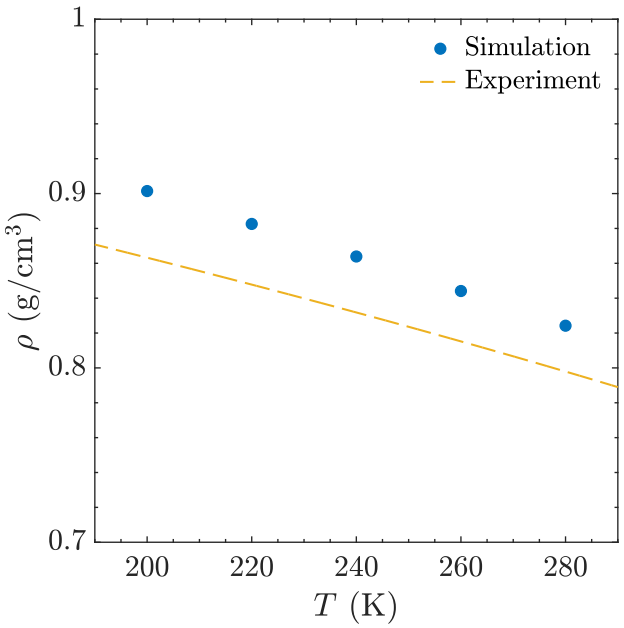

FIG. S1. Comparison between density of 2-propanol as a function of temperature obtained by our simulation and experiment values from Dortmund Data Bank [1].

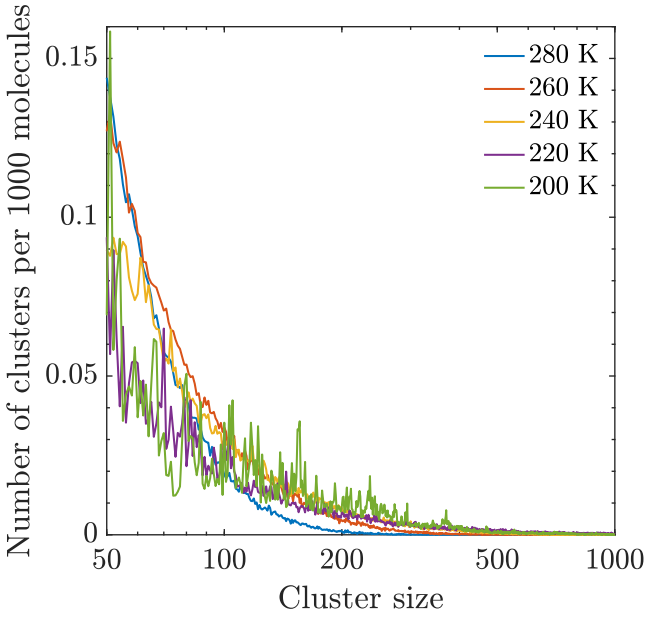

FIG. S2. Size distributions of the supramolecular clusters formed by hydrogen bonding from 50 to 1000 at temperatures ranging from 280 K to 200 K.

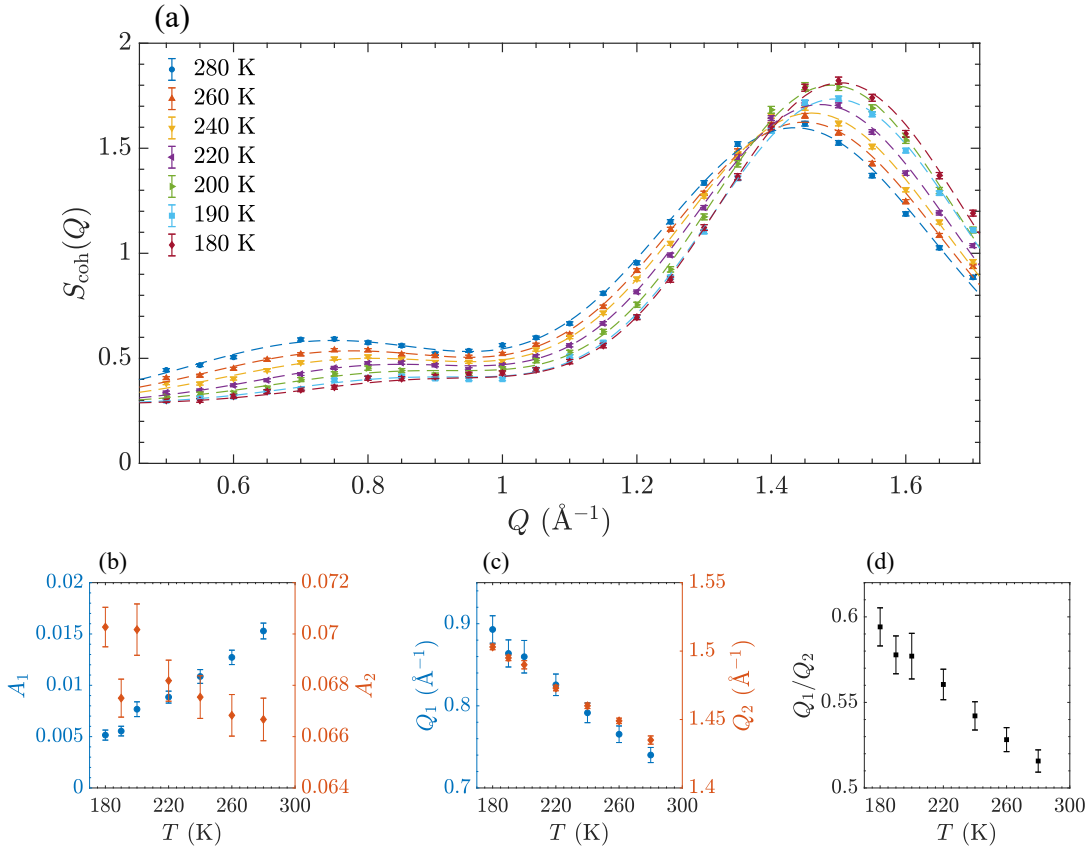

FIG. S3. (a) Coherent structure factor of 2-propanol from 180 K to 280 K measured by polarized neutron diffraction and fitted with two Gaussian functions plus a fixed background of 0.0282. (b) Temperature dependence of the area under the structure factor pre-peak (A_1) and main peak (A_2). (c) Temperature dependence of the positions of the structure factor pre-peak (Q_1) and main peak (Q_2). (d) Ratio between the positions of the structure factor pre-peak and main peak as a function of temperature.

Figure S3 demonstrates the coherent structure factor of deuterated 2-propanol measured by polarized neutron diffraction fitted by two Gaussian functions representing the two scattering peaks, respectively, plus a background, as

$$S_{\mathrm{coh}}(Q) = \frac{A_1}{\sqrt{2\pi\sigma_1^2}} e^{-\frac{(Q-Q_1)^2}{2\sigma_1^2}} + \frac{A_2}{\sqrt{2\pi\sigma_2^2}} e^{-\frac{(Q-Q_2)^2}{2\sigma_2^2}} + \mathrm{bkg} \tag{S1}$$

The background was fixed as 0.0282 as the lowest value (at 190 K) obtained from a beforehand global fit.

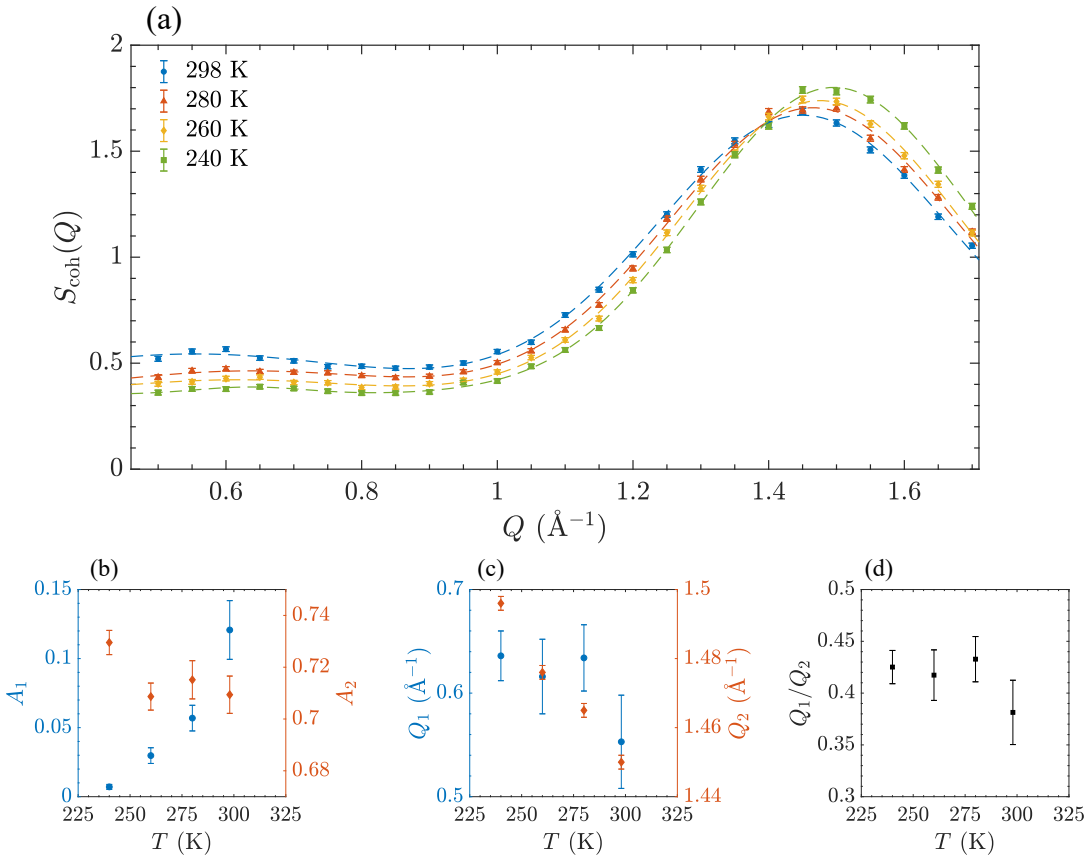

FIG. S4. (a) Coherent structure factor of 1-propanol from 240 K to 298 K measured by polarized neutron diffraction and fitted with two Gaussian functions plus a fixed background of 0.0196. (b) Temperature dependence of the area under the structure factor pre-peak (A_1) and main peak (A_2). (c) Temperature dependence of the positions of the structure factor pre-peak (Q_1) and main peak (Q_2). (d) Ratio between the positions of the structure factor pre-peak and main peak as a function of temperature.

Figure S4 demonstrates the coherent structure factor of deuterated 1-propanol measured by polarized neutron diffraction fitted by Equation S1. The background was fixed as 0.0196 as the lowest value (at 240 K) obtained from a global fit beforehand.

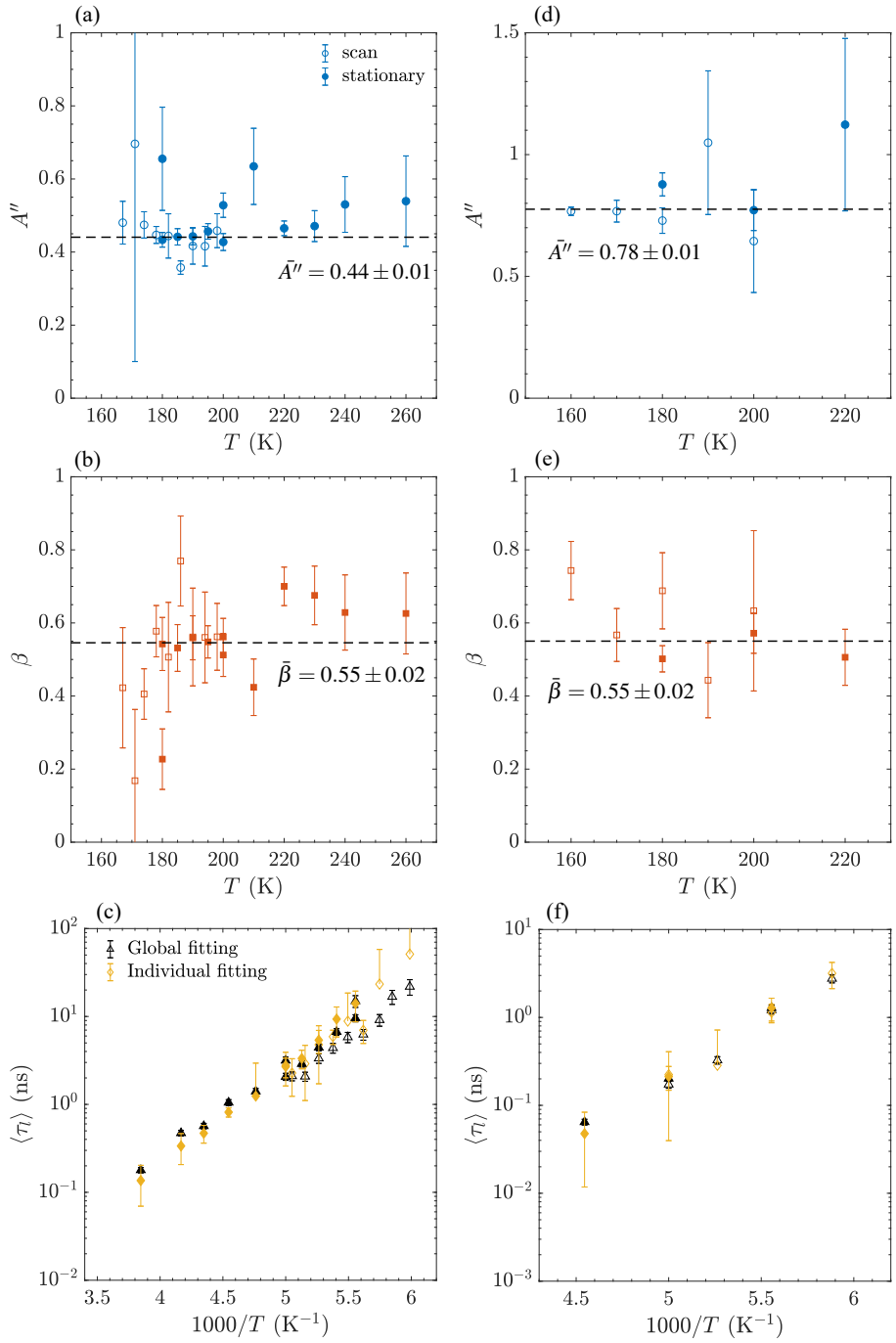

FIG. S5. Individual fitting parameters A'', β and $\langle \tau_l \rangle$ of NSE data by Equation 10 at the structure factor (a-c) pre-peak and (d-f) main peak. The average values of A'' and β are indicated by the dash lines. Global fitting parameters τ, with A'' and β temperature independent, are shown in (c) and (f) for comparison.

TABLE S1. Fitting parameter τ obtained from the global fit for the NSE data at the structure factor pre-peak and χ^2 for each temperature. The upper script "s" indicates the scan mode measurement. Global fitting parameters are $A'' = 0.431 \pm 0.006$ and $\beta = 0.65 \pm 0.02$.

T (K)	167^s	171^s	174^s	178^s	180	180	182^s	185	186^s	190	190^s
τ (ns)	15.94	12.24	6.66	4.56	10.92	6.99	4.24	4.88	3.20	3.24	2.44
$\Delta\tau$ (ns)	3.10	2.14	0.95	0.59	1.56	0.55	0.53	0.35	0.38	0.22	0.28
χ^2	0.8718	2.277	0.7710	0.2963	2.033	1.604	1.680	1.674	2.080	1.336	1.731
T (K)	194^s	195	198^s	200	200	210	220	230	240	260	
τ (ns)	1.51	2.11	1.53	2.30	1.51	1.03	0.77	0.41	0.34	0.13	
$\Delta\tau$ (ns)	0.16	0.13	0.16	0.20	0.12	0.06	0.05	0.02	0.02	0.01	
χ^2	1.628	0.9306	0.7018	2.281	1.050	3.835	2.314	2.641	3.581	2.025	

TABLE S2. Fitting parameter τ obtained from the global fit for the NSE data at the structure factor main peak and χ^2 for each temperature. The upper script "s" indicates the scan mode measurement. Global fitting parameters are $A'' = 0.81 \pm 0.01$ and $\beta = 0.56 \pm 0.01$.

T (K)	160^s	170^s	180	180^s	190^s	200	200^s	220
τ (ns)	7.415	1.657	0.770	0.725	0.196	0.121	0.104	0.039
$\Delta\tau$ (ns)	0.797	0.142	0.033	0.056	0.015	0.005	0.008	0.002
χ^2		1.438	1.440	3.151	1.482	0.8576	1.422	1.741	1.671

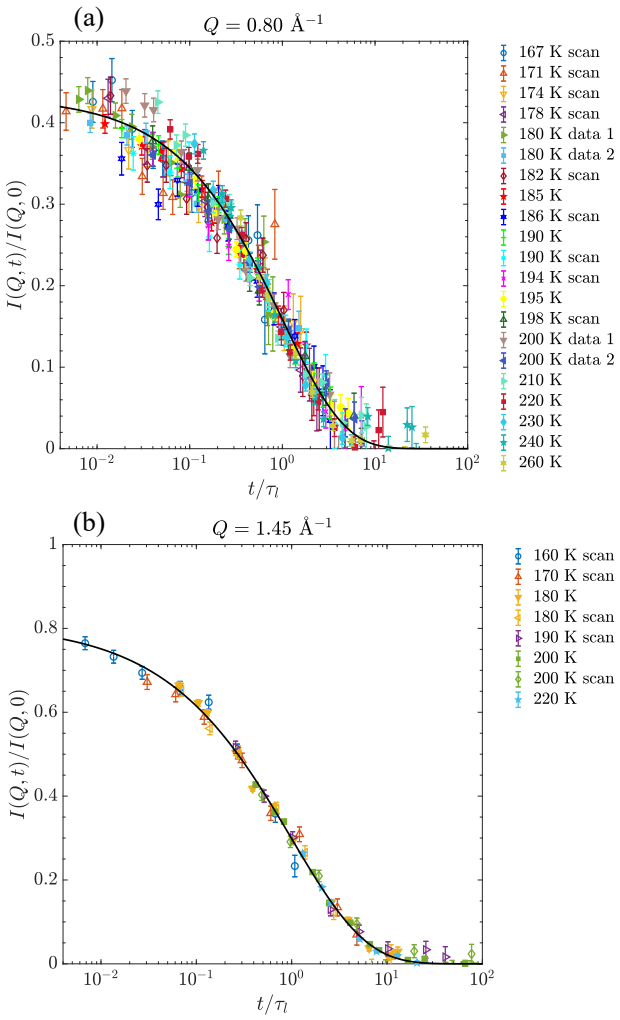

FIG. S6. NSE data with t scaled by τ_l fitted globally according to Equation 10 at the structure factor (a) pre-peak and (b) main peak. The master curves $I(Q,t)/I(Q,0) = A'' \exp(-x^{\beta})$ where $x = t/\tau_l$ are indicated by the solid lines.

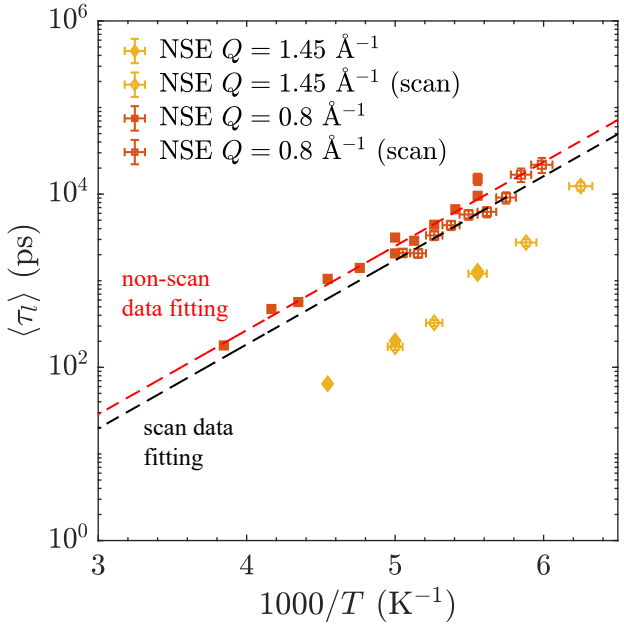

FIG. S7. Arrhenius plot of the average relaxation time measured by QENS measurements at temperature ranging from liquid state to supercooled liquid state using the nominal temperature recorded by the temperature controller. At the prepeak, agreement between the scan and stationary data can be obtained by a constant shift in $1000/T$ corresponding to 0.169 K^{-1} (corresponding to $\approx$ 6 K at 180 K), due to a lack of thermal equilibration in the sample. The main text reports the results shifted accordingly. At the main peak, such shift is not necessary.

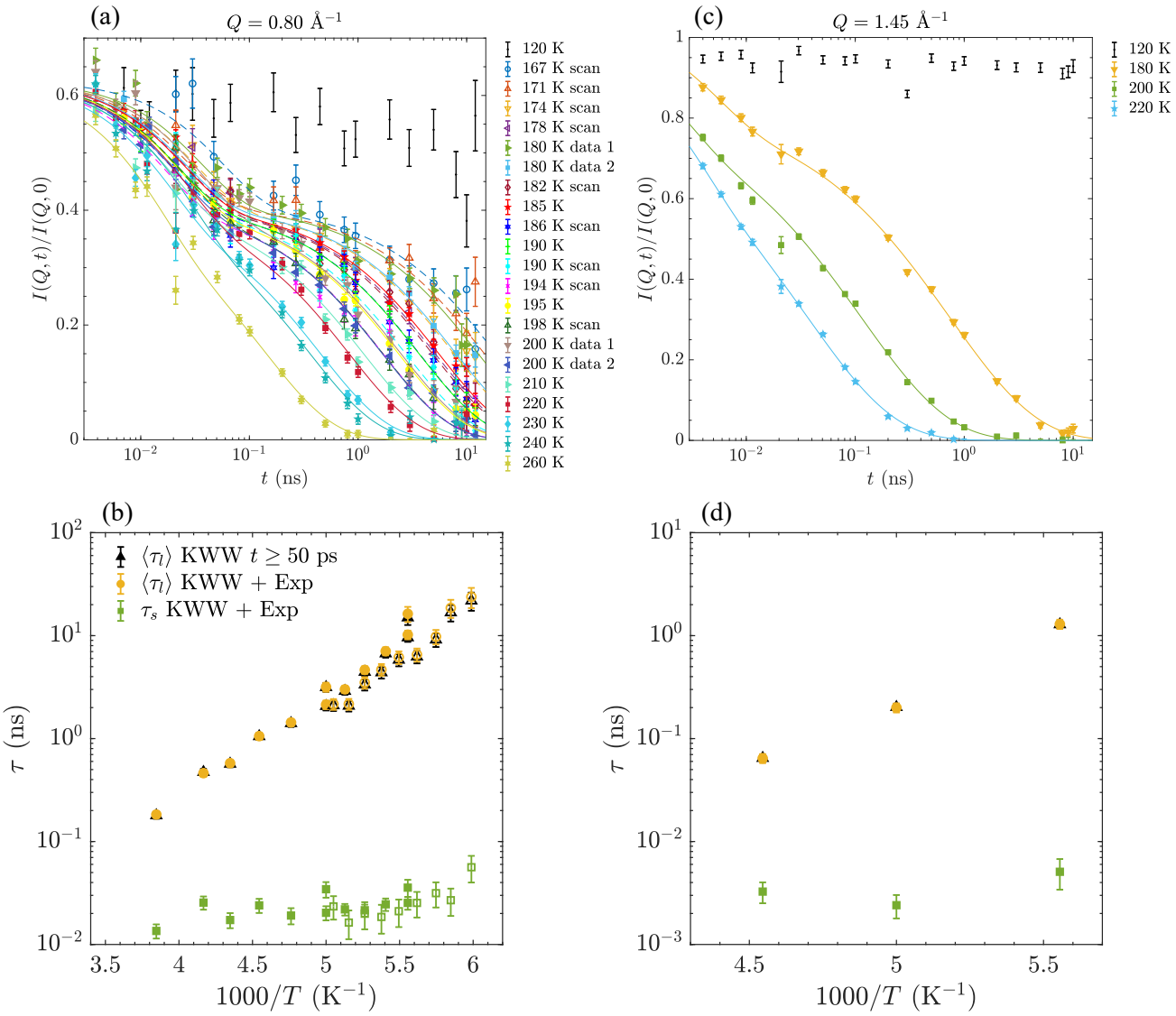

FIG. S8. Global fit for (a) all NSE data at the structure factor pre-peak and (c) the non-scan data at the main peak by Equation 8 with A, A' and β fixed to be equal for all temperatures. (b) and (d) Comparison between fitting parameters τ_l from Equation 10 and τ_l and τ_s from Equation 8. The global fitting parameters are $A' = 0.626 \pm 0.008$, $A = 0.65 \pm 0.01$, and $\beta = 0.69 \pm 0.02$ at the pre-peak, and $A' = 1.06 \pm 0.07$, $A = 0.78 \pm 0.05$, and $\beta = 0.54 \pm 0.02$ at the main peak.

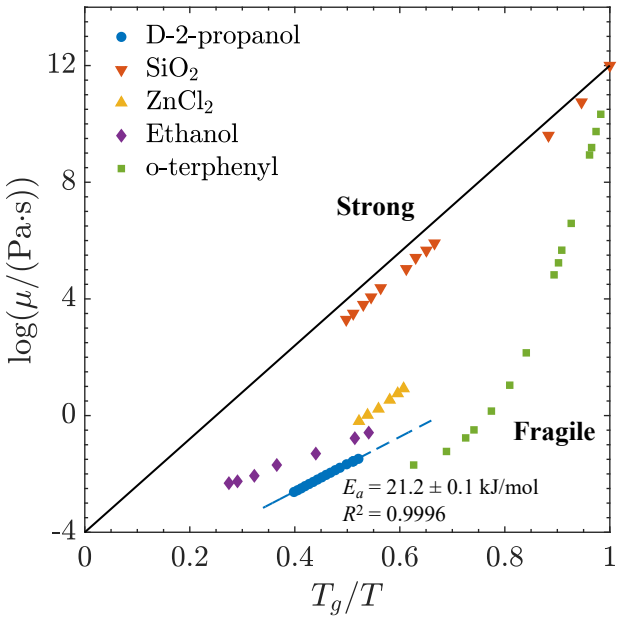

FIG. S9. Dynamic viscosity of deuterated 2-propanol and other examples of strong and fragile glass former (silica, zinc chloride, ethanol, and o-terphenyl) as functions of inverse temperature. An Arrhenius fit of D-2-propanol is indicated by the dash line. The corresponding activation energy is determined to be (21.2 ± 0.1) kJ/mol with $R^2 = 0.9996$. Viscosity values are obtained from the reference [2].

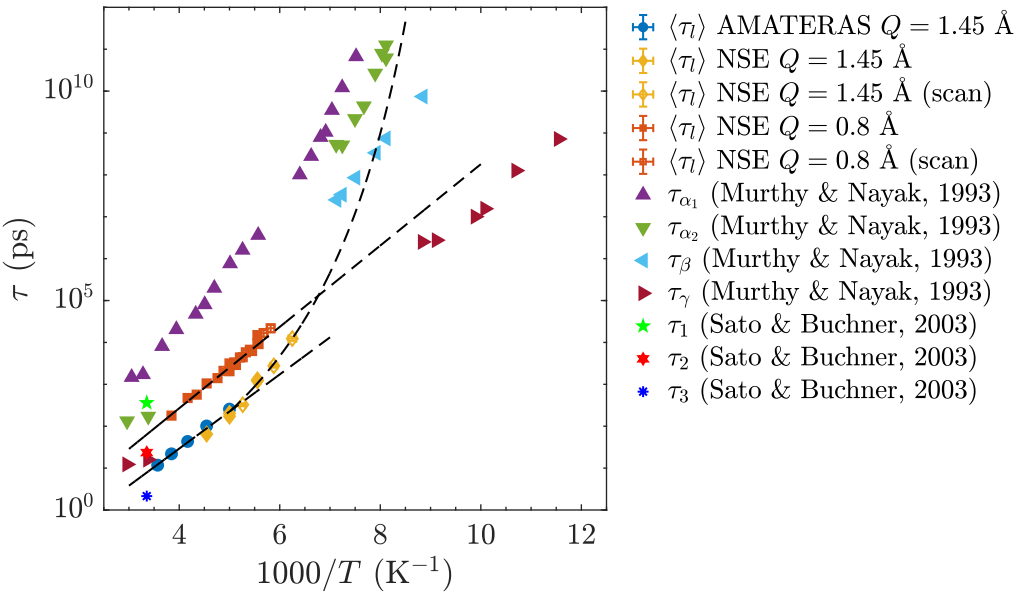

FIG. S10. Comparison between average relaxation time measured by the present neutron scattering experiments and the dielectric measurements performed by Murthy et al. [3] and Sato et al. [4]. The fits of the QENS and NSE data at the main peak and pre-peak are shown as the dash lines.

DISCLAIMER

Uncertainties and error bars throughout the SI represent the confidence interval of one standard deviation.

---

[1] Dortmund Data Bank, http://www.ddbst.com (2021).
[2] V. Lubchenko and P. G. Wolynes, Annual Review of Physical Chemistry **58**, 235 (2007).
[3] S. S. N. Murthy and S. K. Nayak, The Journal of Chemical Physics **99**, 5362 (1993).
[4] T. Sato and R. Buchner, The Journal of Chemical Physics **118**, 4606 (2003).